Research of Pattern Formation, edited by R. Takaki, pp. 389–400.

Dynamics of Cellular Pattern in Two Dimensions

Tatsuzo NAGAI* and Kyozi KAWASAKI**

**Physics Department, Kyushu Kyoritsu University, Kitakyushu 807, Japan*
***Department of Physics, Faculty of Science, Kyushu University 33, Fukuoka 812, Japan*

Abstract. Computer simulations of two-dimensional cellular pattern growth found in coarsening soap froths and grain aggregates have been carried out employing the vertex model. Since the vertex model describes cellular structure and its dynamics by means of the minimal number of degrees of freedom it enables us to simulate systems with large number of cells and definitely gives asymptotic behaviors of the infinite system. It is shown that the vertex model reproduces main characteristics of cellular pattern growth and that it has considerable flexibility for modification.

1. Introduction

Cellular structures are ubiquitous in nature. They range from microscopic scale to macroscopic scale, such as grain texture in polycrystals, magnetic domain structure in magnets, cell texture in biology, soap froths, cellular pattern in Benard convection, columnar joint of basalt, celluar structure of the universe, and so on. Our purpose is to find universal laws underlying formation of those patterns irrespective of space and time.

Grain texture in polycrystals and soap froths have been studied most systematically among others so far (Atkinson, 1988; Weaire and Rivier, 1984). Pattern formation in these systems is driven by the thermodynamic force which attempts to minimize interfacial energy. Their main characteristics are as follows:

(i) Power law growth

The average radius (or size) of cell $\overline{R}(t)$ has the following asymptotic form at long times t

$$\overline{R}(t) = K_0 t^{\nu}, \tag{1.1}$$

where K_0 and ν are positive constants.

(ii) Scaling

The cellular pattern evolution shows a scaling behavior in the time region of the power law growth (scaling regime). Namely, statistical properties of the system are time-invariant if they are rescaled by the length unit of the average cell size.

The exponent of growth law ν is theoretically expected to be 0.5, while the experimental results scatter from 0.25 to 1.0. The scattering of experimental values is likely to come from the fact that secondary effects, e.g. due to impurities, influence the motion of vertices and furthermore that statistical accuracies of experiments are insufficient. Many runs of experiment under the same condition will give a definite result with a high accuracy.

The scaling behavior can be seen by means of the distribution of cell sizes and that of the number of cell edges. The distribution function of cell sizes has the following form in the scaling regime:

$$g(R,t) = \frac{1}{\overline{R}(t)} g^*\left(\frac{R}{\overline{R}(t)}\right), \tag{1.2}$$

where R is a cell size. It was reported that the scaling function $g^*(x)$ is the log-normal distribution function at least in three dimensions, but its verification was not sufficient in two dimensions (Anderson *et al.*, 1989). In order to determine the scaling function with a high accuracy, we need to observe cellular patterns at short time intervals for long times in the large system. The distribution function of the number of cell edges becomes stationary in the scaling regime:

$$f(n,t) = f^*(n), \tag{1.3}$$

where n is the number of cell edges. Equation (1.3) directly expresses that the topology of the system is statistically invariant in time in the scaling regime. Definite forms of $f^*(n)$ and $g^*(x)$ are still unknown.

Computer simulations have played so far the main role in theoretical studies of this problem. In order to overcome the difficulty mentioned above, we need a simple model which still retains the essentials of cellular pattern growth and enables us to simulate development of large systems of cells for long enough periods of time. As examples of such models, we have proposed the so-called vertex models

in two and three dimensions (Nagai *et al.*, 1988; Kawasaki *et al.*, 1989a, 1989b). Computer simulation studies of these models have demonstrated that they are efficient simulation models which reproduce the main characteristics of cellular pattern growth mentioned in Section 1 (Nakashima *et al.*, 1989). In this paper we review a two-dimensional vertex model and its simulation results and discuss its refinement.

2. Vertex Model

Two-dimensional cellular pattern is regarded as an assembly of vertices connected to one another by straight cell boundaries, which will be called interfaces hereafter in the vertex model. Development of the system then can be described through movement of vertices. We find that the effective driving force acting on vertices comes from the surface tension which attempts to minimize the total lengths of interfaces and that the effective frictional force acts on each vertex. If the interfacial energy completely dissipates away through friction the equations of motion for vertices can be written as (Kawasaki *et al.*, 1989a).

$$\sum_{j}^{(i)} \boldsymbol{D}_{ij} \cdot \left(\boldsymbol{v}_i + \frac{1}{2} \boldsymbol{v}_j \right) = -\sum_{j}^{(i)} \sigma \hat{\boldsymbol{r}}_{ij} , \tag{2.1}$$

where $\boldsymbol{D}_{ij}$ is the tensorial friction coefficient given by Eq. (2.2) below, $\boldsymbol{v}_i$ is the velocity of the vertex i, σ the interfacial energy per unit length, $\hat{\boldsymbol{r}}_{ij}$ the unit vector directed from j to i and the sums are over three neighboring vertices j directly connected to the vertex i. The tensorial friction coefficient in Eq. (2.1) is given by

$$\boldsymbol{D}_{ij} = \frac{\sigma}{3L} |\boldsymbol{r}_{ij}| \boldsymbol{n}_{ij} \boldsymbol{n}_{ij} , \tag{2.2}$$

where L is the Onsager kinetic coefficient, $\boldsymbol{r}_{ij}$ the relative vector directed from j to i and $\boldsymbol{n}_{ij}$ the unit normal vector of the interfacial segment $<ij>$. The left hand side in Eq. (2.1) denotes the frictional force acting on the vertex i while the right hand side denotes the driving force. Since the friction coefficient is a tensor a vertex does not necessarily move in the direction of the resultant of three driving forces acting on it.

Furthermore, the two-dimensional vertex model describes topological changes of two-dimensional cellular pattern by means of the two types of elementary processes as follows: when an interfacial segment becomes shorter than a small distance Δ the recombination of vertices, the so-called T1 process, or the annihilation of a triangular cell, the so-called T2 process, occurs depending on whether the interfacial segment in question belongs to none of triangular cells or not, as

shown in Fig. 1.

This vertex model enables us to simulate the large cellular system efficiently because it substantially reduces the number of degrees of freedom by coarse-graining the original cellular system. This will be shown in Section 3.

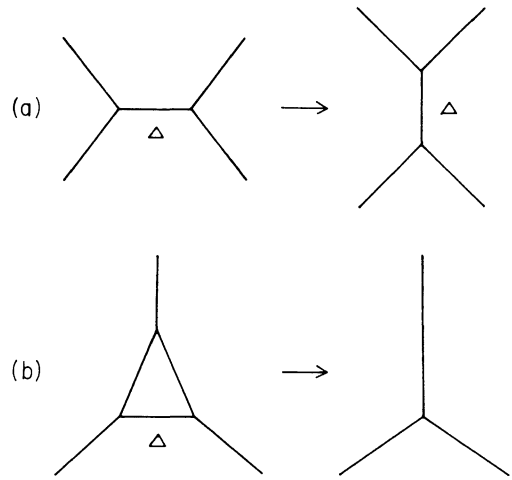

Fig. 1. Elementary processes. (a) Recombination. (b) Triangular annihilation. Δ is the small distance.

3. Computer Simulation

We solve Eq. (2.1) numerically under the periodic boundary condition and choose the Voronoi cell network which contains 48,000 vertices in a rectangular system as the initial state (Nakashima *et al.*, 1989). We monitor the lengths of all the interfacial segments in the system at each step of time. If any segment becomes shorter than the small distance Δ it undergoes either of two types of the elementary processes shown in Fig. 1. We take $\Delta = 0.2$ as the small distance and $\delta t = 0.01$ as the step size of time which are expressed in the length unit $\overline{R}(0)$ and the time unit $\overline{R}(0)^2/L$ where $\overline{R}(0)$ is the initial average size of cell. Tracking the development of the system from $t = 0$ to $t = 100$ we have found the following behavior of the system: after $t \sim 2$ it shows a random pattern different from the initial Voronoi pattern and grows in a statistically similar fashion. Figure 2 shows a snapshot of the pattern obtained in this simulation at $t = 2$. The average size of cells behaves as Eq. (1.1) with $\nu = 0.5$ and the two distribution functions, Eqs. (1.2) and (1.3), approach those shown in Figs. 3 and 4. In these figures the solid lines give our results and the dot-dashed lines are the Monte Carlo results for the Potts model (Glazier *et al.*, 1989). Our distribution functions are slightly sharper than those for the Potts model.

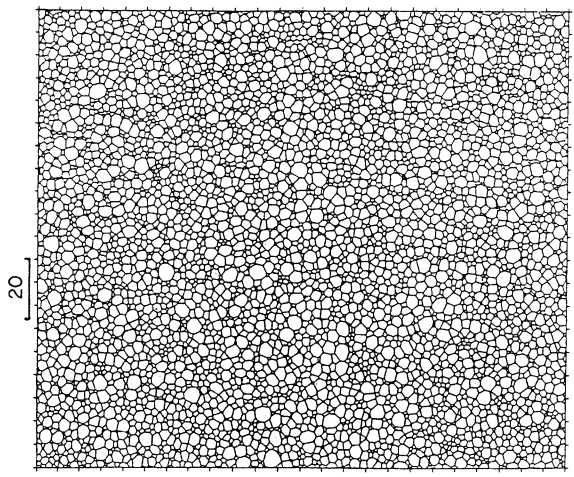

Fig. 2. Snapshot of evolving cellular pattern at $t = 2$.

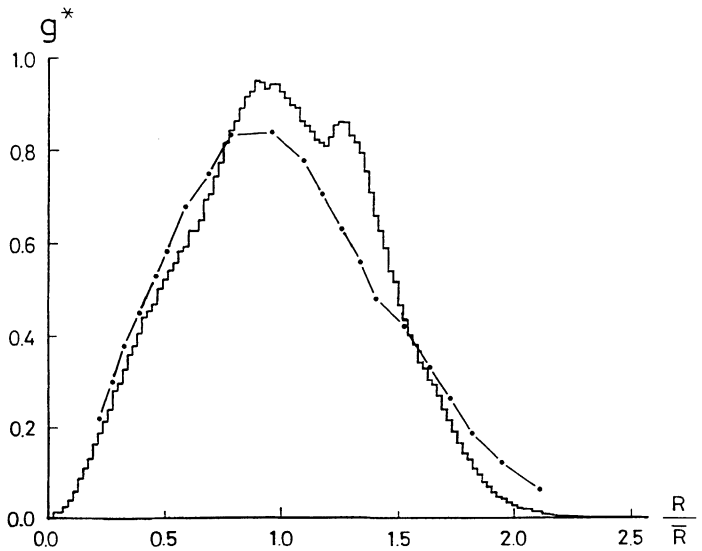

Fig. 3. Distribution of cell sizes in the scaling regime. The solid line shows the simulation result for the original vertex model and the dot-dashed line shows the Monte Carlo simulation result for the Potts model.

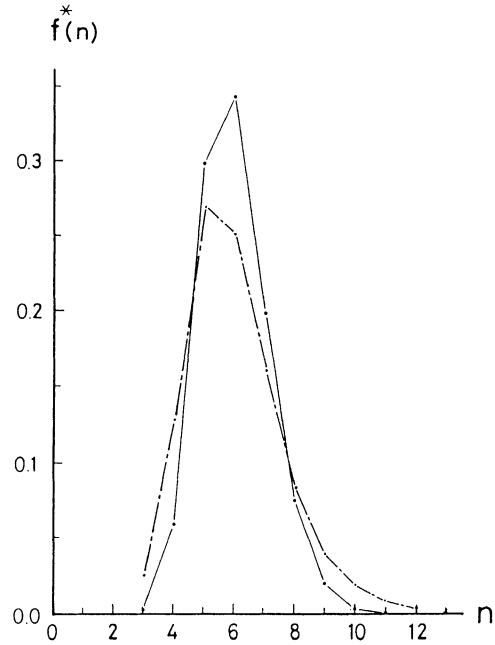

Fig. 4. Distribution of the number of cell edges in the scaling regime. The solid line shows the simulation result for the original vertex model and the dot-dashed line shows the Monte Carlo simulation result for the Potts model.

4. Modified Vertex Model

The crucial point of the vertex model mentioned in Section 3 is to assume straight interfaces instead of the original curved ones. We here try to include the effects of finite curvature of interfaces in the vertex model and examine how the results mentioned in Section 3 are modified (Kawasaki *et al.*, 1990; Nagai and Kawasaki, 1990).

The generally accepted picture of cellular pattern growth is based on the following equation for the normal velocity of interface at a point s:

$$v(s) = LK(s), \tag{4.1}$$

where L is the Onsager kinetic coefficient and $K(s)$ the local curvature. The velocity $v(s)$ points to the center of the radius of curvature. Each vertex is the terminus of three such interfaces meeting at equal angles of $2\pi/3$ radians. From the viewpoint of the vertex model we are not so much interested in the motion of the three

interfaces as in the resulting motion of the vertices. Therefore, we here modify Eq. (2.1) in such a way that the equations of motion for vertices in the vertex model correctly reproduce the vertex motion in the picture mentioned above. Namely we write the modified equation as

$$\sum_j^{(i)} \boldsymbol{D}_{ij} \cdot \left(\boldsymbol{v}_i + \frac{1}{2}\boldsymbol{v}_j \right) = -\sum_j^{(i)} \sigma C\left(\theta_j\right)\hat{\boldsymbol{r}}_{ij}. \tag{4.2}$$

Here we have introduced a correction function $C(\theta_j)$ where θ_j is the angle between the two interfaces other than the interfacial segment $<ij>$ emerging from the vertex i and is illustrated in Fig. 5. In fact finite curvature must influence both the frictional force and the surface tension, although apparently we only correct the latter in Eq. (4.2). However, this correction factor must already include the modification of the frictional force.

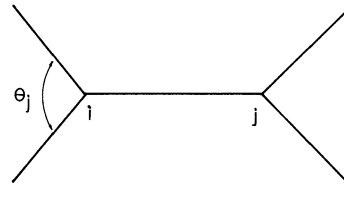

Fig. 5. Definition of the angle θ_j.

As was already mentioned, the correction function $C(\theta)$ is determined in such a way that Eq. (4.2) gives the correct velocity of vertex. Since it is difficult to do so generally we consider the following symmetric configuration of vertices: an n-sided regular polygon connected to n outer fixed vertices by symmetrically radiating straight lines. Equation (4.2) then gives rise to the outward component of the vertex velocity given by

$$v = B_{\mathrm{M}}(n)\frac{L}{a}, \tag{4.3}$$

where a is the edge length of n-sided regular polygon and

$$B_{\mathrm{M}}(n) = \left\{ C\left(\pi - \frac{2\pi}{n}\right) - 2C\left(\frac{\pi}{2} + \frac{\pi}{n}\right)\sin\left(\frac{\pi}{n}\right) \right\} \cos^{-2}\left(\frac{\pi}{n}\right). \tag{4.4}$$

We consider two cases, soap froths and grain aggregates, for the symmetric configuration. In these cases the movements of interfaces obey Eq. (4.1) and three curved interfaces meet at equal angles of $2\pi/3$ radians at each vertex. We assume in the case of soap froths that interfaces are circular arcs and obtain analytically the velocity of vertex in the symmetric configuration. In the case of grain aggregates, we numerically track the movements of an interfacial segment and a corresponding vertex in the symmetric configuration. Then we obtain the velocity of vertex given by Eq. (4.3) where $B_M(n)$ is replaced by

$$B_S(n) = -\frac{4}{\sqrt{3}}\sin(\pi x) \quad \text{for soap froths} \tag{4.5}$$

and

$$B_G(n) = b_1 x + b_2 x^2 + b_3 x^3 \quad \text{for grain aggregates,} \tag{4.6}$$

where $x \equiv 1/n - 1/6$, $b_1 = -7.26$, $b_2 = -4.43$, $b_3 = 8.44$. Here the length a in Eq. (4.3) is defined as the distance between the two neighboring vertices. The difference between $B_S(n)$ and $B_G(n)$ is small in the whole range of the edge number $3 \le n < \infty$ $(-1/6 < x \le 1/6)$.

The correction function $C(\theta)$ can be determined by the equation $B_M(n) = B_S(n)$ for soap froths and the equation $B_M(n) = B_G(n)$ for grain aggregates. Here we use $x = 1/n - 1/6$ as a continuous variable and numerically solve the above functional equations for $C(\theta)$ by expanding them into series with respect to x. The results are plotted in Fig. 6 as functions of the angle $\theta = 2\pi \times (1/3 - x)$ for $0 < \theta < \pi$, where the region of variables is extended from the discrete space of n to the continuous space of θ. In Fig. 6 the solid curve shows the correction function for soap froths while the dotted curve shows that for grain aggregates. The modification is remarkable for small angles, while there is no modification at $\theta = 2\pi/3$ which corresponds to a regular hexagon. Thus, we can say that the effect of finite curvature is most important for triangles corresponding to $\theta = \pi/3$ and that it prevents shrinking of triangular cells.

We expect that the correction functions obtained above are applicable to general random configurations of cells, although they have been derived for the symmetric configuration. This is because it can be expected that this symmetric configuration well describes the average behavior of a cell in the scaling regime. In fact we found that the rate of change of the area A_n of an n-sided cell, dA_n/dt, which is analytically calculated using Eq. (2.1) for this configuration reproduces well the corresponding quantity for the average area $\overline{A}_n$, $d\overline{A}_n/dt$, obtained by the computer simulation mentioned in Section 3.

We now perform computer simulations by using Eq. (4.2) with the correction function given in Fig. 6. Here we choose the number n of cell edges instead of the

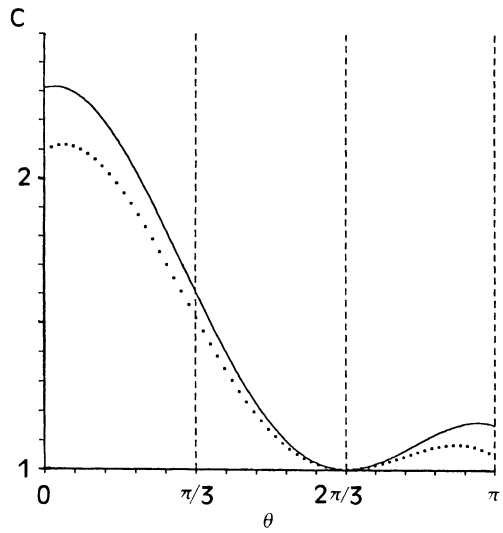

Fig. 6. Correction function. The solid curve is for soap froths and the dotted curve is for grain aggregates.

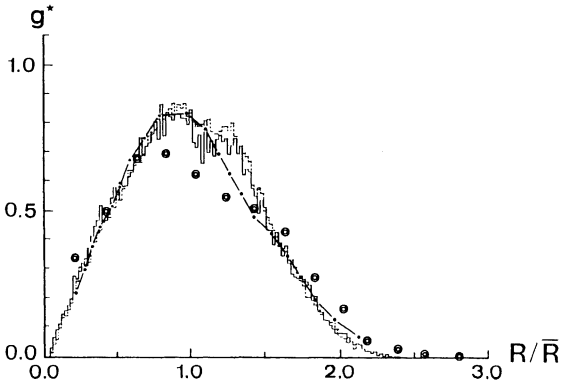

Fig. 7. Distribution of cell sizes in the scaling regime. The solid line and the dotted line show the simulation results for the modified vertex model in the cases of soap froths and grain aggregates, respectively. The dot-dashed line shows the Monte Carlo simulation result for the Potts model. The double circles are the experimental results for the two-dimensional soap froth.

angle θ between two interfaces at each vertex where we use the relation $\theta = \pi - 2\pi/n$ for an n-sided regular polygon. The simulation method is the same as that explained in Section 3. The initial number of vertices is 6,000 and 100 runs have been performed. The system shows the scaling behavior in the almost same region

of time as in the previous one. The growth exponent is unchanged, i.e. $\nu = 0.5$. Figures 7 and 8 show the results for the distribution of cell sizes and that of the number of cell edges, respectively, in the scaling regime. The solid line and the dotted line give our results for soap froths and for grain aggregates, respectively, in both figures. The difference in two distributions between the two systems is small. The two distributions have become broad compared with those for the original vertex model shown in Figs. 3 and 4 and are closer to the Monte Carlo results for the Potts model shown by the dot-dashed lines (Glazier *et al.*, 1989). The experimental results are also plotted in both figures using the circles (Simpson *et al.*, 1967) and the double circles (Glazier *et al.*, 1989) for two-dimensional soap froths and the squares (Simpson *et al.*, 1967) for a two-dimensional grain aggregate. We can say that the agreement between the experimental results and our results for the modified vertex model is satisfactory as a whole, since the accuracy of the experimental results cited above seems not to be sufficient. Many experimental runs should be carried out under the same condition because statistical fluctuations are large due to finiteness

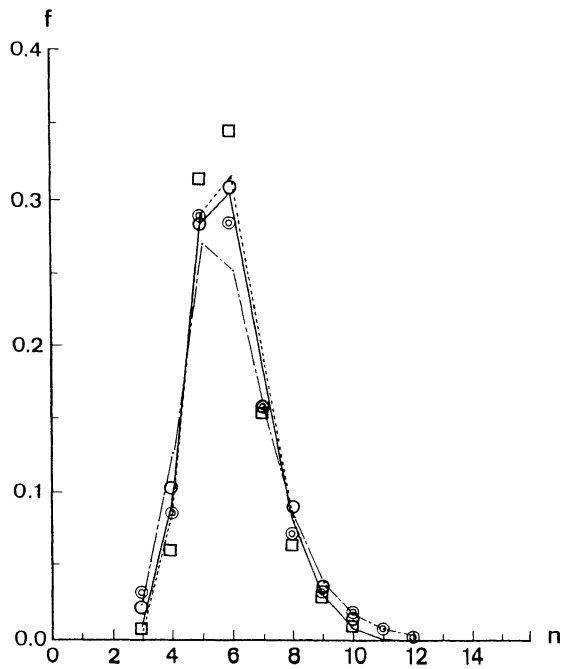

Fig. 8. Distribution of the number of cell edges in the scaling regime. The solid line and the dotted line show the simulation results for the modified vertex model in the cases of soap froths and grain aggregates, respectively. The dot-dashed line shows the Monte Carlo simulation result for the Potts model. The single circles and the double circles are the experimental results for the two-dimensional soap froths and the squares are those for the two-dimensional grain aggregates.

of the system in the cellular pattern growth. Our simulation results given above are the values that are averaged over 10 time points in the scaling regime in each run and over 100 runs. We should notice that one can further refine the vertex model by employing the angle variable instead of the number of cell edges for the correction function.

5. Conclusion

We have carried out computer simulations of two-dimensional cellular pattern using the vertex model. The cellular pattern is regarded as an assembly of vertices connected to one another through straight interfaces in this model. We have shown that the effects of finite curvature of interfaces can be included in this model. As a result, we conclude:

(1) The two-dimensional vertex model is efficient to simulate the system containing the large number of cells. The modified vertex model reproduces the experimental results and the other simulation results.
(2) Effects of finite curvature of interfaces are remarkable especially for triangular cells. This means that it is important to treat the motion of triangular cells properly.
(3) The effects of finite curvature of interfaces are absent for the growth law.
(4) Finite curvature of interfaces tends to broaden the distribution of cell sizes and that of the number of cell edges.

The two-dimensional vertex model has been extended to the three-dimension and the computer simulation for the latter is in progress (Kawasaki *et al.*, 1989b; Nagai *et al.*, 1990).

REFERENCES

Anderson, M. P., Grest, G. S., and Srolovitz, D. J. (1989), Computer Simulation of Normal Grain Growth in Three Dimensions, Phil. Mag., **B59**, 293–329.

Atkinson, H. V. (1988), Theories of Normal Grain Growth in Pure Single Phase Systems, Acta Metall., **36**, 469.

Glazier, J. A., Anderson, M. P., and Grest, G. S. (1989), Coarsening in the Two Dimensional Soap Froth and the Large Q Potts Model: A Detailed Comparison, preprint.

Kawasaki, K., Nagai, T., and Nakashima, K. (1989a), Vertex Models for Two-dimensional Grain Growth, Phil. Mag., **B60**, 399–421.

Kawasaki, K., Nagai, T., and Nakashima, K. (1989b), Statistical Physics of Domain Walls and Grain Boundaries in Ordering Kinetics, in Cooperative Dynamics in Complex Physical Systems, edited by Takayama, H., Springer-Verlag, Heidelberg.

Kawasaki, K., Nagai, T., and Okuzono, T. (1990), Time Evolution of Random Cellular Patterns, in Microscopic Aspect of Nonlinearity in Condensed Matter, edited by Tognetti, V., Plenum, New York.

Nagai, T., Kawasaki, K., and Nakamura, K. (1988), Vertex Dynamics of Two-dimensional Cellular Patterns, J. Phys. Soc. Jpn., **57**, 2221–2224.

Nagai, T. and Kawasaki, K. (1990), Simulations of Vertex Models for Grain Growth, in Proceedings of NRIM International Workshop on Computational Materials Science.

Nagai, T., Ohta, S., Kawasaki, K., and Okuzono, T. (1990), Computer Simulation of Cellular Pattern Growth in Two and Three Dimensions, Phase Transitions, **28**, 177–211.

Nakashima, K., Nagai, T., and Kawasaki, K. (1989), Scaling Behavior of Two-dimensional Domain Growth: Computer Simulation of Vertex Models, J. Stat. Phys., **57**, 759–787.

Simpson, C. J., Beingessner, C. J., and Winegard, W. C. (1967), Similarities between Grain Growth in Metals and Organic Plastic Crystals, Trans. Metall. Soc. AIME, **239**, 587–588.

Weaire, D. and Rivier, N. (1984), Soap, Cells and Statistics-Random Patterns in Two Dimensions, Contemp. Phys., **25**, 59–99.